SSC24-P2-27

Concept and Feasibility of Enabling Broadband Communication to a Remote Sensing Satellite

Fong-Yu Chen and Chieh-Fu Chang

Taiwan Space Agency
8F., No. 9, Zhanye 1st Rd., East Dist., Hsinchu City 300091 , Taiwan (R.O.C.); +886-3-5784208#9482
bell.chen@tasa.org.tw

ABSTRACT

Traditional remote sensing satellites uses X-band transmitter (XTX) to dump large volume of image data in a high data rate, i. e., greater than 100Mbps. Since the need and trend of low-earth-orbit (LEO) communications arise, we wonder if we can improve the usefulness of a remote sensing satellite by upgrading the inherent XTX as a X-band transceiver (XTRX), so that a remote sensing satellite can incorporate additional broadband communication functionality. This work investigates the feasibility in three perspectives with the illustration of FORMOSAT-8, an optical remote sensing satellite.

First, from the perspective of antenna and RF chain, the downlink band remains at 8.025GHz to 8.4GHz and the uplink band is selected at 7.9GHz to 7.95GHz. In this case, transmission band and receiving band are not too far so that a well-defined horn antenna can cover both bands. Besides, a diplexer is added to separate the receiving signal from the transmission signal. Secondly, from the perspective of baseband processing and intermediate scheme, i. e., sampling, digital-to-analog and analog-to-digital converters (DAC/ADC), due to the progress of software defined radio (SDR) and the availability of FPGA, the flexibility of reconfiguration from the processing of a simplex transmitter to that of a duplex transceiver is affordable since the cost and risk of schedule are greatly reduced. Thirdly, from the perspective of system, the size, weight and power consumption (SWaP) of FORMOSAT-8 (FS8) are investigated and discussed. The technology of steerable solar panel is also suggested to attain sufficient electrical power when simultaneously adjusting the attitude for the X-band antenna to point at the ground terminal.

Finally, the telemetry and telecommand (TM/TC) communication can be moved to X-band and thus the traditional S-band module and the associated antenna can be neglected. Furthermore, in order to implement TMTC and broadband communication in the same band efficiently, a scheme of packet switching is suggested. The scheme also applies when multiple ground users exist.

1. INTRODUCTION

FORMOSAT-8 (FS8) is Taiwan optical remote sensing satellite. It consists of 6 satellite and each satellite will be launch sequentially from 2025 to 2030. The major mission is capturing images from space and transmitting them back to Earth. It consists of a number of units: Solar Array (SA)、Power Control Unit (PCU), On Board Computer (OBC), Electronic Unit (EU), Focal Plane Assembly (FPA), Reaction Control System (RCS), GPS receiver, Star Tracker, Thermal Control System (TCS), Attitude and Orbit Control System (AOCS), and Communication Unit, which includes two subsystems: S-band and X-band [1].

S-BAND SUBSYSTEM

The Telemetry (TM) and Telecommand (TC) subsystem is responsible for bidirectional communication between the satellite and the ground station. This subsystem maintains the contact between ground station and the satellite. The central frequency of uplink is 2039.645833 MHz, with BPSK modulation and data rate of 4 kbps. The central frequency of downlink is 2215.000000 MHz with BPSK modulation and data rate of 2 Mbps. The satellite's body-mounted S-band antennas consist of two different types: Flat panel antenna and Helical antenna as shown in Figure 1 and Figure 2, respectively. The block diagram of S-band subsystem is provided in Figure 3 [2].

Figure 1: Flat panel antenna [3]

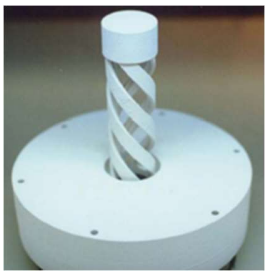

Figure 2: Helical antenna [3]

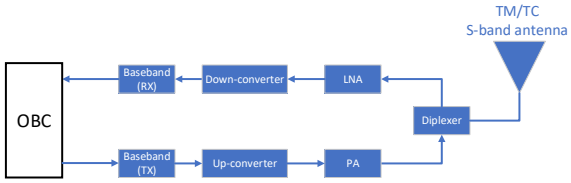

Figure 3: FS8 satellite S-band architecture

X-BAND SUBSYSTEM

The X-band downlink subsystem transmits optical payload data to the ground and its central frequency is 8200 MHz. The data rate is 500 Mbps. The satellite's body-mounted transmitting antenna is a horn as shown in Figure 4. The block diagram of the X-band subsystem is shown in Figure 5 [4].

Figure 4: Horn antenna [3]

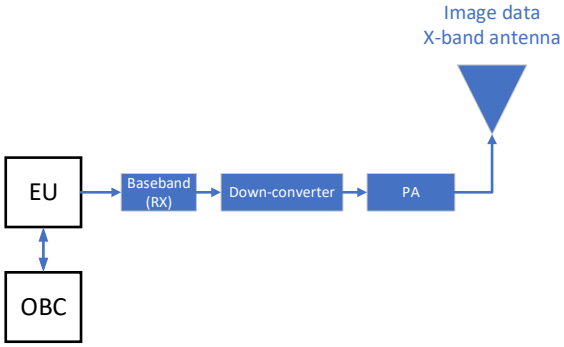

Figure 5: FS8 satellite X-band architecture

The overall structure including OBC with S-band and X-band subsystems are provided in Figure 6.

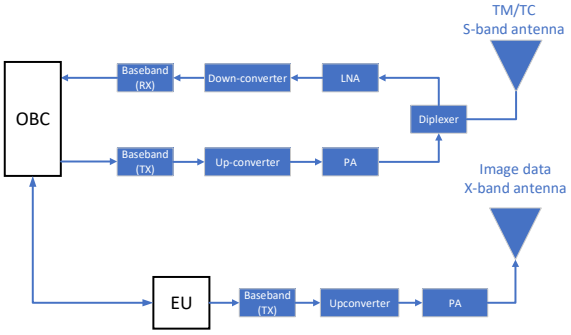

Figure 6: S-band & X-band in the FS8 satellite architecture

In this work, we try to modify X-band subsystem so that duplex broadband communication can be enabled in the original remote sensing satellite. The sole idea is to

modify the original XTX as a XTRX. Two additional advantages can be gained by this modification:

1. TM/TC can be shifted to X-band, which fits the future trend that TM/TC in S-Band become extremely crowded because of the huge growth of LEO (Low Earth orbit) satellites in recent years [5] [6].

2. Spaceborne mass data storage can be attained for not only downloading, but also uploading. It will become clear later.

2. COMMUNICATION SYSTEM

THE ORIGINAL AND PROPOSED STRUCTURE

The original X-band downlink subsystem include a transmitter operating at the frequency range 8040 MHz ~8360 MHz. It transmits the image data of the optical payload to the ground station as shown in Figure 7. Note that the band-passed filter (BPF) is a cavity having sharp edge to greatly suppress out-of-band emission and complying with the high-rate spectral mask adopted by Space Frequency Coordination Group (SFCG) [7].

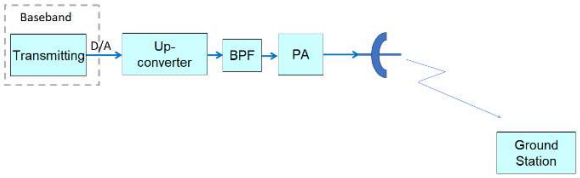

Figure 7: The original X-band downlink subsystem.

Next, in order to fulfill our motivation, we modify the transmitter as a transceiver so that it can both transmit and receive signal as shown in Figure 8. From Figure 8, we add a diplexer and a receiving chain. From the perspective of hardware, our transmitter and receiver can share the original antenna. A significant advantage is that we do not need to change the structure of FS8, which is already quite compact. In order to achieve this, we add a diplexer and select the receiving band as 7900MHz ~ 7950MHz. Since the receiving band is close to the transmitting band, the characteristics of antenna can readily remain. Note that because both baseband processing of the transmitter and the receiver can be implemented in an FPGA, not only regenerative mode, but also bent-pipe mode can be implemented easily, i. e., the sampled data from ADC of the receiver can be switched to as input bit stream to the DAC of the transmitter.

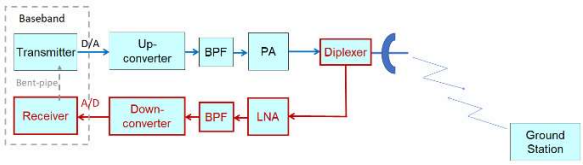

Figure 8: The proposed X-band communication subsystem.

CHARACTERISTICS OF ANTENNA AND ISOLATION ISSUE [4]

First, the antenna is a horn and the gain is shown in Figures 9 and Figures 10 for left-handed circular polarization (LHCP) and right-handed circular polarization (RHCP), respectively.

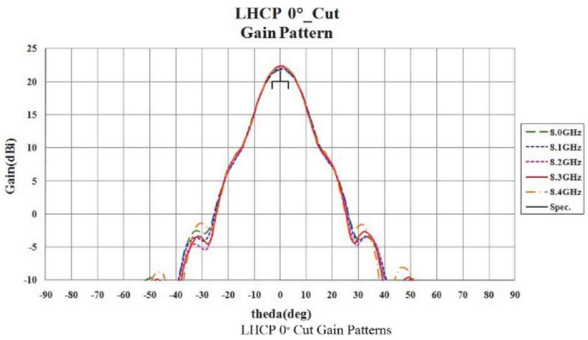

Figure 9: LHCP Antenna gain

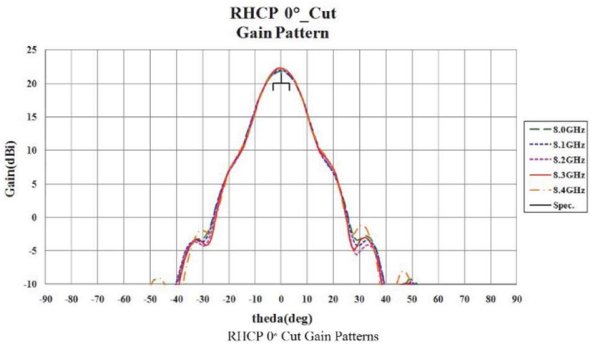

Figure 10: RHCP Antenna gain

Next, because the receiving band is close to the transmitting band, we need to pay attention to the isolation. The original transmitting end adopts LHCP whose return loss and isolation are shown in Figure 11 and Figure 12, respectively. The added receiving end adopts RHCP whose return loss and isolation are shown in Figure 13 and Figure 14, respectively.

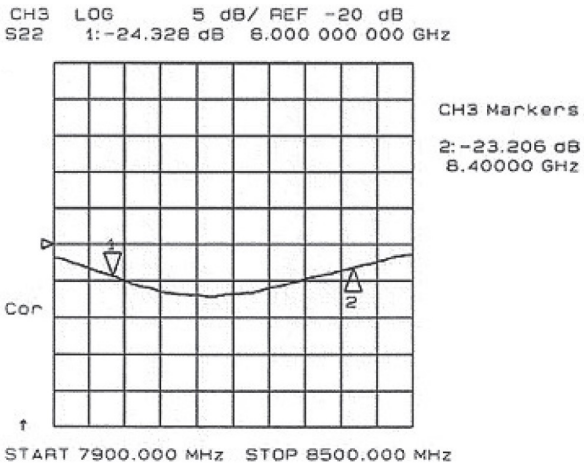

Figure 11: LHCP Return loss of the horn antenna

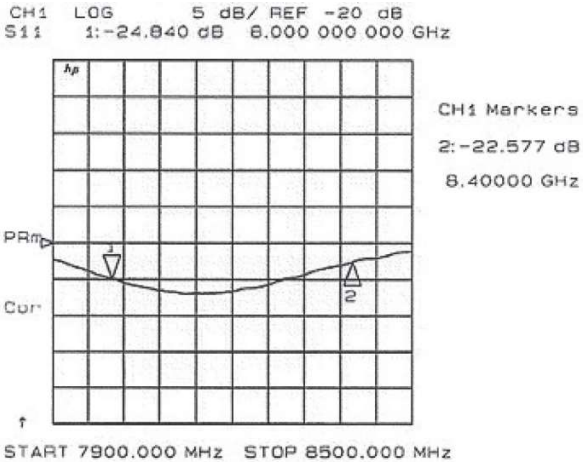

Figure 13: RHCP Return loss of the horn antenna

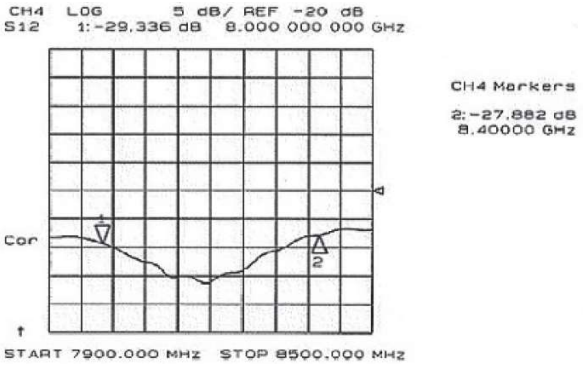

Figure 12: LHCP Isolation of the horn antenna

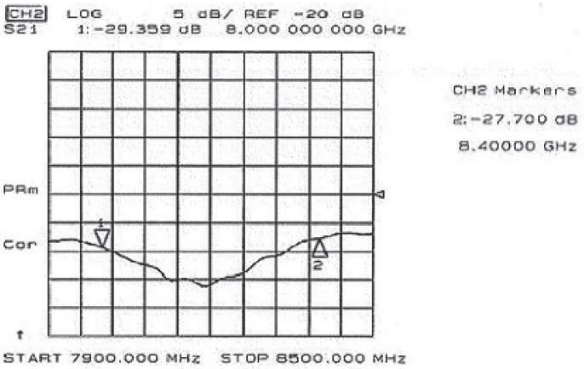

Figure 14: RHCP Isolation of the horn antenna

As we can see from Figure 12 and Figure 14, the isolation of circular polarization is greater than 25dB. In addition, it is important to mention that the cavity BPF greatly improves the isolation between the transmitting chain and receiving chain because of the sharp edge to significantly suppress the out-of-band emission and comply with the spectral mask of SFCG [7][8].

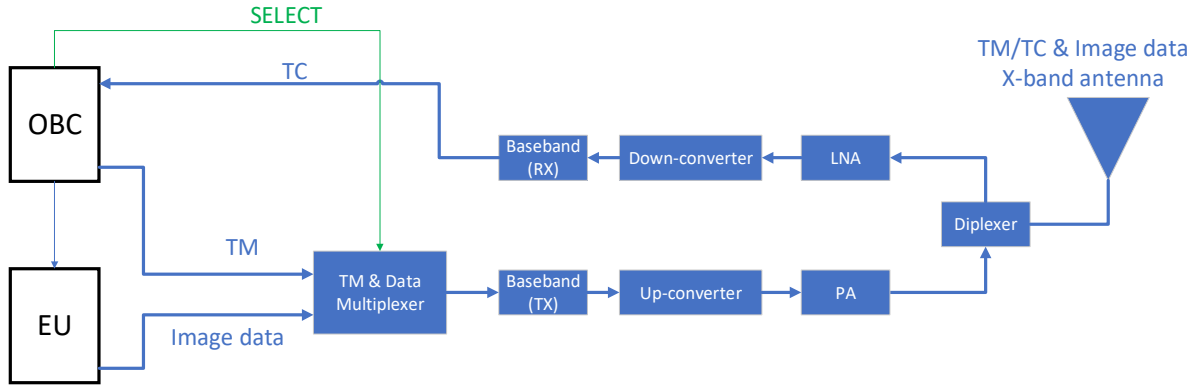

Figure 15: Satellite X-band architecture diagram for TM/TC & Image data

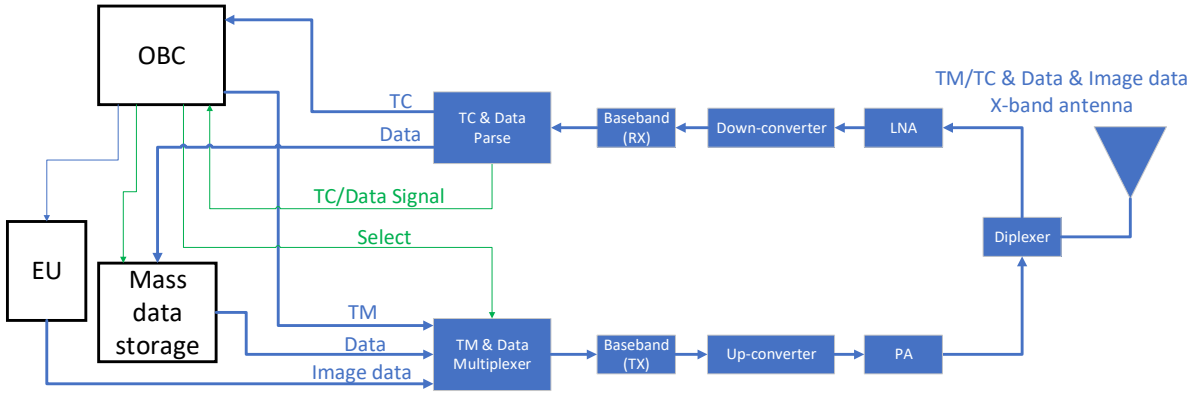

Figure 16: Satellite X-band architecture diagram for TM/TC & Mass data & Image data

INCORPORATING TMTC AND REMOVING S-BAND MODULE

In recent years, the emergence of LEO satellite constellations for both communications and sensing has made spectrum crowded, especially for traditional S-band as TMTC (TM: 2200MHz~2290MHz; TC: 2025MHz~2120MHz). In our approach, we can further modify the original communication subsystem architecture to incorporate TMTC function as shown in Figure 15. By doing so, we can remove the original S-band module to save space, weight and power consumption. Because the modified architecture merges TM/TC communication, ground stations upload TC to the satellite via X-band, while the satellite downloads TM such as satellites state of health to the ground.

It is worth to mention that the modified communication subsystem in Figure 15 has an interesting potential application: by adding a channel between the receiver and the original mass storage for the payload data as shown in Figure 16, the communication module can serve as a data storage center in space! It allows data to be uploaded to the satellite and stored. Hence the modified structure in Figure 16 enables the original mass storage to have more diverse usage. However, the sharing of mass storage with original optical payload data is the cost and we need to make sure the storage resource is sufficient for us to do so.

SCENARIO OF MULTIPLE USERS

In case of multiple users, because the uplink communication may probably burst frames (mainly for commanding), we suggest to adopt frequency division multiple access (FDMA). On the other hand, the downlink communication may mainly consecutive frames and in some scenarios, only one or a few users may dominate the usage. For example, a user requests a desired payload image data. Hence we suggest to adopt the scheme of packet switching in order to utilize the great downlink bandwidth efficiently.

3. FEASIBILITY REGARDING SWAP

POWER

The orbit period of the FS8 satellite is approximately 95.88 minutes, with a sunlight shading duration of 34.38 minutes. The solar panels receive sunlight for approximately 58.5 minutes. The overall power supply provided by the solar panels is shown in Table 1 [9].

Table 1 The power generated from solar panels.

Solar array power (Normal mode)	
Orbit average power	Daylight average power
202.12WH (6.73AH)	335.31WH (11.177AH)

The battery capacity is 18AH. Under the original architecture, the estimated power generation and consumption for the entire satellite is provided in Table 2 [10][11].

Table 2 The overall power generation and consumption

Solar power acquired / orbit	202.12WH (6.73AH)
Spacecraft power used / orbit	181.73WH (6.057AH)
Margin (Battery efficiency loss included)	+4.69%

In this work, we focus on the communication system and its power consumption is provided in Table 3.

Table 3 The power consumption of the original communication system

Item	Power (W)	Power (AH)	Duty (/orbit)	Total power (/orbit)
S-band transmitter	15W	0.1145	22.9%	0.3095AH
S-band receiver	4.5W	0.15	100%	
X-band transmitter	40W	1.3333	10%	

After the modification, the S-band transmitter and S-band receiver are removed, while the X-band transmitter is retained and an X-band receiver is added. We estimate that the power consumption of the X-band receiver will be 40% of the X-band transmitter's power consumption. The estimated power consumption is in shown in Table 4.

Table 4 The estimated power consumption of the modified communication system

Item	Power (W)	Power (AH)	Duty (/orbit)	Total power (/orbit)
X-band receiver	16W	0.5333	100%	0.8266AH
X-band transmitter	40W	1.3333	22.9%	

The total power consumption difference between before and after the architecture modification is given by

$$(\text{After change}) - (\text{Before change}) = (\text{Difference})$$

$$0.8266\text{AH} - 0.3095\text{AH} = 0.5171\text{AH} \qquad (1)$$

Hence the change of margin is given by

$$\frac{(\text{Difference})}{(\text{Battery capacity})} = (\text{Margin change})$$

$$\frac{0.517}{18\text{AH}} = 2.87\% \quad (2)$$

From Table 2 and Eq. (2), the overall power margin after modification is given by

$$(\text{Original margin}) - (\text{Margin change}) = (\text{Newly margin})$$

$$+4.69\% - 2.87\% = +1.82\% \quad (3)$$

From above, the power margin decreases but still positive after the modification of the communication system.

WEIGHT AND SIZE

Comparing with Figure 7 and Figure 8, for the proposed structure, we need to add the receiving chain: an X-band diplexer, band-passed filter and down-converter. The estimated weight of the three components is 1.9kg. Since the satellite weights around 390kg, the increasing weight is about 0.5%. Besides, when we further consider the structure in Figure 16 saving S-band module [2], including a transceiver unit, diplexer and antennas as shown in Figure 7, the overall weight actually decreases and is less than 390kg. Similarly, since we neglect S-band module, the overall size slightly decreases.

CONCLUSION AND DISCUSSIONS

The major task of current FORMOSAT-8 satellites is to take images of the earth and transmit the data through X-band to the ground. In our work, we propose a slightly modified structure as shown in Figure 8 so that X-band transmitter becomes a transceiver and the high data rate uplink is enabled. Besides, we further incorporate TMTC functionality into X-band communication so that S-band module can be saved. The saving of the weight and size with an affordable slight increase of power consumption justify the feasibility of our idea. Furthermore, we hope this work may benefit other remote sensing satellite programs so that the functionality of high data rate uplink can be added to the satellites with a slight modification.

Finally, it is worth to mention that the emergence of LEO satellite systems, mainly for both communications and remote sensing, makes the orbit and spectrum crowded, and naturally motivates the integration of sensing and communications [12][13]. Our work coincides with the trend but from a different perspective.

Acknowledgments

The authors would like to express gratitude to Dr. I-Young Tarn and TASA for all the support.

References

[1] TASA technical report, "FORMOSAT-8 Satellite Structure Design Report – Delta CDR," FS8-RPT-0010, 2020.

[2] TASA technical report, "FORMOSAT-8 S-Band TT&C Subsystem Design Report," FS8-RPT-0122, 2020.

[3] TASA FORMOSAT-8 public information, https://www.tasa.org.tw/en-US/missions/detail/FORMOSAT-8

[4] TASA technical report, "FORMOSAT-8 XDS Design Report," NSPO-RPT-0071, 2020.

[5] NASA technical report, "X-Band CubeSat Communication System Demonstration", doc. number 20160001365, 2016.

[6] F. Delhaise, etc., "LISA Pathfinder and X-Band Telemetry, Telecommand and Tracking Support in Near-Earth Phase", SpaceOps Conference, 2016.

[7] "Radio frequency and modulation", ECSS-E-ST-50-05-C, 2011. https://ecss.nl/standard/ecss-e-st-50-05c-rev2-radio-frequency-and-modulation-4-october-2011/

[8] TASA technical report, "FORMOSAT-8 X-band Cavity Filter Baseline Functional Test Record," FS8-PROC-3067_02-T01, 2022.

[9] TASA technical report, "FORMOSAT-8 Solar Array Specification," FS8-SPEC-0047, 2021.

[10] TASA technical report, "FORMOSAT-8 Battery Component Specification," FS8-SPEC-0046, 2019.

[11] TASA technical report, "FORMOSAT-8 EPS Design Reports," FS8-RPT-0068, 2020.

[12] L. Yin, etc., "Integrated Sensing and Communications Enabled Low Earth Orbit Satellite Systems," IEEE Network arXiv, 2024.

[13] F. Liu, etc., "Joint radar and communication design: Applications, state-ofthe-art, and the road ahead," *IEEE Transactions on on Communications*, vol. 68, no. 6, pp. 3834–3862, 2020.